Simultaneous Control of Ionic and Electronic Conductivity in Materials: Thallium Bromide Case Study

Cedric R. Leão* and Vincenzo Lordi†

Lawrence Livermore National Laboratory, Livermore, California, 94550, USA

(Received 5 December 2011; published 15 June 2012)

Achieving simultaneous control of ionic and electronic conductivity in materials is one of the great challenges in solid state ionics. Since these properties are intertwined, optimizing one often results in degrading the other. In this Letter, we propose a method to limit ionic current without impacting the electronic properties of a general class of materials, based on codoping with oppositely charged ions. We describe a set of analyses, based on parameter-free quantum mechanical simulations, to assess the efficacy of the approach and determine optimal dopants. For illustration, we discuss the case of thallium bromide, a wide band gap ionic crystal whose promise as a room-temperature radiation detector has been hampered by ionic migration. We find that acceptors and donors bind strongly with the charged vacancies that mediate ionic transport, forming neutral complexes that render them immobile. Analysis of carrier recombination and scattering by the complexes allows the identification of specific dopants that do not degrade electronic transport in the crystal.

DOI: 10.1103/PhysRevLett.108.246604 PACS numbers: 72.60.+g, 66.30.Dn, 71.55.Cn, 72.20.Jv

Long after solid-state electronics had been mastered, triggering one of the most important technological revolutions in history, the discovery of fast ion conductors (FICs) in the 1960s made possible the development of whole new classes of devices. FICs found applications in energy storage and conversion with the creation of lithium ion batteries and fuel cells using solid electrolytes, as well as gas sensors based on zirconia, which are present in virtually every automobile produced worldwide [1]. Since response times for sensors or better charge/discharge rates in batteries depend on the ionic current, the ability to enhance it is highly desirable. This can be achieved by the incorporation of supervalent elements into the host material [1–3]. The charge imbalance introduced by dopants in ionic materials is usually compensated by the formation of oppositely charged vacancies, which results in an increase of ionic current. This is the case for Ti-doped $NaAlH_4$ used for hydrogen storage [4], Zr-doped CeO_2 used for catalysis or gas sensors [2], and transition metal-doped $LiFePO_4$ used for ion battery cathode [3], to mention some examples. However, manipulating the ionic conductivity of FICs often affects their electronic properties, which one might want to independently control. For example, in solid electrolytes for batteries or fuel cells the electronic conduction must be suppressed, whereas it must be kept at metallic levels for electrodes or logic switches [5,6]. The opposite also occurs when dopants meant to improve the electronic properties of a material impair the optimal ionic conductivity [7]. The inability to coordinate ideal ionic and electronic properties is a great challenge that precludes the implementation of several materials in technological applications.

In this Letter, we tackle the general problem of how to reduce the ionic current in materials without impacting their electronic properties. This is desirable for a wide class of mixed conductors. We illustrate our approach with thallium bromide (TlBr), a promising material for high-performance room-temperature gamma- and x-ray detection [8,9]. Its performance, however, invariably degrades after operation times that vary from hours to several weeks [10]. This phenomenon, termed polarization, is associated with an ionic current in the crystal when electrically biased, leading to the accumulation of charged ions at the device's electrical contacts. Several ways to circumvent this problem have been attempted, including ultrapurification [11], operation at low temperatures [12], using Tl contacts [13], employing surface treatments [14], engineered device geometry [15], and making larger crystals [16]. None of these techniques, however, solve the polarization problem indefinitely.

We propose a new approach for reducing ionic current through the introduction of supervalent dopants that form neutral pairs with the electrically charged vacancies, since the mechanism for ionic migration is mediated by vacancies (or at least facilitated by them in materials with Frenkel defects). Strongly bound, neutral vacancy–dopant pairs are less mobile than the vacancies alone, as experimentally demonstrated at low temperatures for many ionic crystals doped with one element [1,17,18]. Above about room temperature, materials doped with supervalent ions exhibit higher ionic current relative to the pristine ones, as discussed above, because the presence of supervalent ions induces the formation of an equal number of new vacancies. Therefore, to reduce the ionic current it is necessary to avoid the formation of new vacancies. This is possible by simultaneously codoping with ions of excess negative (A) and positive (D) charge relative to the host ions (Br^- and Tl^+, respectively), as indicated by the

 © 2012 American Physical Society

following defect reactions in the Kröeger-Vink notation:

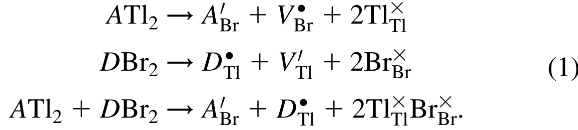

$$\begin{aligned} A\mathrm{Tl}_2 &\rightarrow A'_{\mathrm{Br}} + V^{\bullet}_{\mathrm{Br}} + 2\mathrm{Tl}^{\times}_{\mathrm{Tl}} \\ D\mathrm{Br}_2 &\rightarrow D^{\bullet}_{\mathrm{Tl}} + V'_{\mathrm{Tl}} + 2\mathrm{Br}^{\times}_{\mathrm{Br}} \\ A\mathrm{Tl}_2 + D\mathrm{Br}_2 &\rightarrow A'_{\mathrm{Br}} + D^{\bullet}_{\mathrm{Tl}} + 2\mathrm{Tl}^{\times}_{\mathrm{Tl}}\mathrm{Br}^{\times}_{\mathrm{Br}}. \end{aligned} \quad (1)$$

To demonstrate the approach and assess the results, we used quantum mechanical simulations [19] to model the electronic properties of pristine and doped TlBr (CsCl structure). Calculations were based on density functional theory [21,22] treating the exchange-correlation term with both the generalized gradient approximation as implemented by Perdew, Burke, and Ernzerhof (PBE) [23] and a hybrid exchange-correlation functional (HSE06) [20]. With PBE, we obtained a direct band gap of 1.98 eV (at point X of the Brillouin zone) and a lattice parameter of 4.06 Å for the pristine material, compared to experimental values of 3.01 eV (direct gap) and 3.97 Å, respectively, (at 4.7 K [24]). The HSE06 functional yielded improved results of 2.67 eV and 4.04 Å. Inclusion of spin-orbit coupling shifted the conduction band minimum to point R in both approaches, resulting in an indirect gap of 1.50 eV (PBE) and 2.22 eV (HSE06). Some experiments indicate an indirect band gap of about 2.7 eV for this material, but the transition from the valence band maximum at X to the conduction band minimum at R is forbidden [25]. As pointed out in [26], the excellent electronic properties of TlBr for radiation detectors stem from the very shallow nature of Tl and Br vacancies, whose formation energies cross near the middle of the band gap and pin the Fermi level there, as shown in Fig. S1 in the Supplemental Material [27]. The pinning of the Fermi level near midgap keeps the free carrier concentration low in the intrinsic material, contributing to the low noise and high energy resolution observed in measured radiation spectra (see [28]). The low formation energy of vacancies at the point of Fermi level pinning ($\Delta E_f = 0.4$ eV with PBE and 0.46 eV with HSE06 in the smallest cell), which is a common feature of ionic materials, favors compensation of extrinsic dopants by the mechanism described in Reactions (1) rather than generating free carriers at the band edges.

We modeled Pb, Te, Se, and S dopants in TlBr with $3 \times 3 \times 3$, $4 \times 4 \times 4$, and $5 \times 5 \times 5$ cubic supercells (54, 128, and 250 atoms, respectively). We found that the chalcogens mostly originate either neutral interstitials or negatively charged defects incorporated on Br sites, whereas Pb is positively charged and incorporates on Tl sites. All the dopants were tested on both atomic sites, as well as four nonequivalent interstitial sites. The most favorable configuration was then tested in association with the oppositely charged vacancy. Figure 1 shows the PBE formation energies and charge states of the Pb- and Se-associated defects as a function of the Fermi level. Similar figures for S and Te are available online [27] (Fig. S2). The formation energies were calculated by [29]:

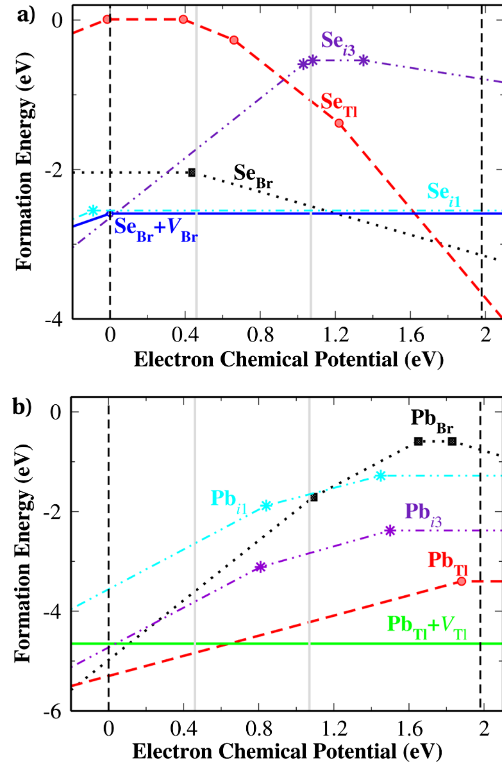

FIG. 1 (color online). Formation energies of Pb (a) and Se (b) defects in TlBr. The lowest energy configuration was tested in association with the oppositely charged vacancy. The slopes of the lines give the charge state of the defects. The vertical dashed lines indicate the calculated positions of the band edges in pristine TlBr, and the vertical solid lines bound the region of the Fermi level in which the formation energies of the vacancies are positive (see Fig. S1 in the Supplemental Material [27]). Stoichiometric conditions were considered.

$$\Delta E_f = E_d - (E_p - n\mu_x) + q(\mu_e + E_{\mathrm{VBM}}), \quad (2)$$

where E_d and E_p are the total energies of the defective and the pristine supercells, respectively, n is the number of atoms of element x removed from the supercell and added to a reservoir whose chemical potential is μ_x, and q is the amount of charge exchanged from a reservoir with electron chemical potential μ_e, which we reference to the energy of the valence band maximum, E_{VBM}. Spurious periodic electrostatic interactions for supercells with charged defects were corrected using the Makov-Payne scheme [30,31]. We neglect in Eq. (2) terms involving the chemical potentials of extrinsic elements because it suffices to know the relative formation energies of different defects associated with each dopant for our purposes. The formation enthalpy of TlBr was evaluated from $\Delta H_f = \mu_{\mathrm{TlBr}} - \mu^B_{\mathrm{Tl}} - \mu^B_{\mathrm{Br}}$, where the superscript B denotes bulk phase. We obtained 1.69 eV with PBE and 1.86 eV with HSE06, both in good agreement with experiment at 1.79 eV [33]. The chemical potentials for Tl and Br ions in the stoichiometric regime are given by $\mu_{\mathrm{Tl(Br)}} = \mu^B_{\mathrm{Tl(Br)}} + \Delta H_f/2$ [28,34]. Results using PBE and HSE06

on $3 \times 3 \times 3$ supercells were in very close agreement for the positions of the charge state transitions relative to the VBM, as shown in Table I in the Supplemental Material [27]. Therefore, we can confidently use the PBE results from the larger supercells, which are better converged with respect to finite-size effects. Inclusion of spin-orbit coupling for the transition levels of both Pb and Se doped material did not change the results.

In Fig. 1 we show that $Pb^{\bullet}_{Tl}$ and Se'_{Br} form neutral complexes with V'_{Tl} and $V^{\bullet}_{Br}$, respectively, indicated by the flat lines. Our calculations show that Se_i in the vicinity of $V^{\bullet}_{Br}$ spontaneously collapse into substitutional defects. The binding energy of a defect complex is given by [35]:

$$\Delta E_{\mathrm{bind}} = E_{\mathrm{complex}} - \sum_i E_{d,i}, \tag{3}$$

where E_{complex} is the formation energy of the defect complex and $E_{d,i}$ are the formation energies of each individual defect comprising the complex. Negative values indicate binding complexes. Table I shows the binding energies of several complexes of interest for intrinsic, Pb and Se doped TlBr [36]. Results for complexes involving Pb in association with S or Te are available in Table II in the Supplemental Material [27], to estimate residual finite-size errors, we compare the results for the three supercells. Schottky pairs in HSE06 calculations bind with an energy of −0.56 eV, again showing the reliability of our PBE results, at −0.54 eV. For additional validation, we calculated the binding energy of Ca_{Tl} with V_{Tl} as −0.34 eV with PBE for the $5 \times 5 \times 5$ supercell in striking agreement with the experimental estimate of −0.36 eV [17].

In Fig. 2, we show two main possibilities for the vacancies to bind to the dopant pairs: each vacancy "bonded" to both dopants (configuration *a*) or each vacancy bonded only to the dopant that has opposite charge to it (configuration *b*). Configuration *a* is more strongly bound by ~0.3, as indicated in Table I. Moreover, these dopants–vacancies complexes bind much more strongly than the Schottky pairs alone (see Table I). Further, complex *a* is bound 0.6 eV more strongly than the sum of pairs involving only a single vacancy and the oppositely charged dopant, and more importantly, 0.5 eV more strongly bound than the sum of an isolated Schottky pair and an isolated pair of dopants. If the latter was the most favorable case, the dopants would not reduce vacancy mobility relative to the intrinsic material. The ionic conductivity varies exponentially with the inverse of the activation barrier, plus the binding energy given in Table I [1]. Therefore, the formation of complexes *a* and *b* shown in Fig. 2 will reduce the mobility of ions much more dramatically than the mere association of Schottky pairs does in pure TlBr.

TABLE I. Binding energies of acceptor-donor complexes, involving or not vacancies in two supercells. Configurations *a* and *b* for the dopant-pair–vacancy-pair complex are shown in Fig. 2.

Complex	Sites	E_{bind} (eV) $4 \times 4 \times 4$	$5 \times 5 \times 5$
$V'_{Tl} + V^{\bullet}_{Br}$ (Schottky pair)	2nd NN	−0.44	−0.36
$Se'_{Br} + V^{\bullet}_{Br}$	2nd NN	−0.54	−0.39
$Pb^{\bullet}_{Tl} + V'_{Tl}$	1st NN	−0.41	−0.37
$Pb^{\bullet}_{Tl} + Se'_{Br}$	1st NN	−0.83	−0.73
$V'_{Tl} + Pb^{\bullet}_{Tl} + Se'_{Br} + V^{\bullet}_{Br}$	config. *a*	−1.46	−1.29
	config. *b*	−1.18	−0.93

The remaining question is whether this suppression of ionic current and consequent stabilization of TlBr comes at the expense of its favorable electronic properties. We can generally characterize the electronic properties in terms of the carrier mobilities, μ, and lifetimes of excitations, τ. For the purpose as a radiation detector, we require maximizing μ and τ. For TlBr, τ for electrons is very large, on the order of 10^{-2} s [9]. The main source of degradation of τ would be Shockley-Reed-Hall recombination centers. Because the recombination rate increases exponentially with the difference in energy between an electron or hole trap state and the respective band edge, defects that introduce states near the middle of the band gap are most detrimental. We see in Fig. 1 that only very low concentration (high formation energy) Pb-related defects introduce deep levels, indicated by kinks in the formation energy curves. On Tl sites, Pb impurities are very shallow donors. Se_{Br} shows a $-1/0$ acceptor transition as the material becomes more hole-rich (decreasing μ_e) at $E_{\mathrm{VBM}} + 0.44$ eV. However, this transition occurs outside the allowed region of μ_e between the solid vertical lines in Fig. 1. We confirmed this result using the HSE06 functional, extrapolating to the larger supercell sizes, as shown in Table I in the Supplemental Material [27]. Thus, the trap level would always be filled, not affecting carrier lifetimes. S_{Br} shows a $-1/0$ acceptor transition even farther (> 0.1 eV) in the region of inaccessible Fermi level by both PBE and HSE06 calculations. Te_{Br}, however, exhibits an acceptor transition deep in the gap (0.16 eV inside the allowed Fermi level range by PBE, 0.4 eV by HSE06).

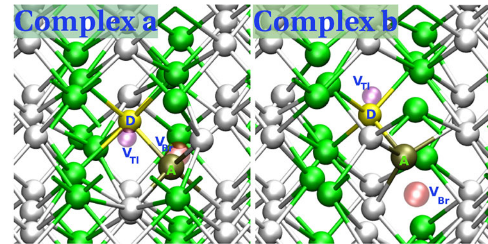

FIG. 2 (color online). Supercells of the TlBr crystal with defect complexes consisting of a donor dopant, D_{Tl} (D=Pb), an acceptor dopant A_{Br} (A=S, Se, or Te), and vacancies. Vacancies V_{Br} and V_{Tl} are indicated by translucent spheres. In configuration *a*, the vacancies are nearest neighbors to both dopants, whereas in configuration *b* they are nearest neighbors only to the oppositely charged dopant.

Therefore, Te dopants are detrimental to carrier lifetimes, but S, Se, and Pb are not.

Carrier scattering in TlBr at room temperature is expected to be dominated by lattice vibrations, since the Debye temperature is only ~160 K [37]. The acoustic phonon limit to the mobility can be approximated by [38]:

$$\mu = \frac{2\sqrt{2\pi}}{3} \frac{e\hbar^4 c_\ell}{m^{5/2}(k_B)^{3/2} D_A^2} T^{-3/2}, \tag{4}$$

where e is the electron charge, $\hbar$ is the reduced Planck's constant, c_ℓ is the longitudinal elastic constant (3.76×10^{10} N/m^2 at room temperature for TlBr [39]), m is the effective mass of the carrier of interest (we obtained $m_e = 0.51m_0$ and $m_h = 0.98m_0$, in good agreement with experimental data, $m_e^{\mathrm{expt}} = 0.55m_0$ and $m_h^{\mathrm{expt}} = 0.82m_0$ [40]), k_B is Boltzmann's constant, T is the lattice temperature, and D_A is the deformation potential computed as described in [41]: −25.67 eV for electrons and −28.14 eV for holes. Using Eq. (4), we calculated the phonon-limited mobility at 300 K as ~19 cm^2/V for electrons and ~3 cm^2/V for holes, in excellent agreement with that measured for high quality material [37]. This agreement indicates that phonon scattering dominates the carrier mobility in TlBr. Given that the requirement is of doping levels on the order of the concentration of intrinsic vacancies (around $10^{15} - 10^{16}$ cm^{-3} for a highly pure crystal) [11,18], the defect complexes discussed above should not affect electronic transport unless they are orders of magnitude stronger scattering centers than the intrinsic defects in the material.

The carrier scattering strength introduced by a defect is given by Fermi's golden rule between two electronic states $\Psi_f(k')$ and $\Psi_i(k)$, with energies ε_f and ε_i. To first order, the scattering rate is given by

$$W_{ij} = \frac{2\pi}{\hbar} |\langle \Psi_f(k')|V_{\mathrm{pert}}|\Psi_i(k)\rangle|^2 \delta(\varepsilon_f - \varepsilon_i), \tag{5}$$

where the perturbation potential $V_{\mathrm{pert}}(\mathbf{r}) = V_d(\mathbf{r}) - V_0(\mathbf{r})$ is the difference between the total self-consistent potential in the defect cell, $V_d(\mathbf{r})$, and the ideal cell, $V_0(\mathbf{r})$. In principle, Eq. (5) must be integrated over a significant number of pairs of states and k points in the Brillouin zone to get the total scattering rate. However, a qualitative measure of the average scattering rate can be obtained from V_{pert} alone via [42]

$$\tilde{M}^2 = \left(\int d\mathbf{r} |\nabla V_{\mathrm{pert}}| \right)^2. \tag{6}$$

In Fig. 3 we show the calculated "relative scattering rates," $\tilde{M}^2$, for the different individual defects as well as the complexes of interest for TlBr. We find that the complexes involving dopants and the two types of vacancies are less than 3 times stronger scattering centers than Schottky pairs. Because scattering by dopant complexes is within an order of magnitude of the intrinsic defect scattering, which is overwhelmed by phonon scattering in undoped TlBr, codoping at levels sufficient to bind a large fraction of naturally occurring vacancies will not degrade carrier mobility relative to the pristine material.

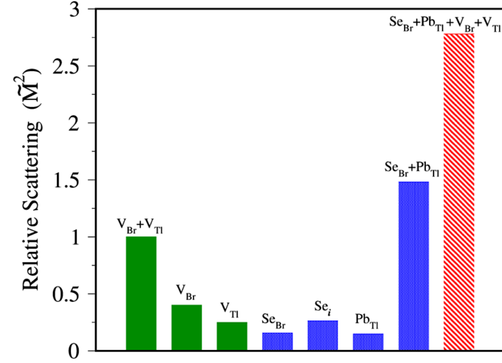

FIG. 3 (color online). Relative carrier scattering strengths of different intrinsic and extrinsic defects and defect complexes in TlBr as given by Eq. (6). The values are normalized to that for the Schottky pair.

In summary, we have described a new method to limit ionic conductivity in a general class of materials without impacting their electronic properties. The approach consists of doping the material with ions supervalent to the host material so that the dopants form neutral complexes with charged vacancies that mediate ionic transport. To prevent the generation of new vacancies to balance the excess charge introduced by the dopants, simultaneous introduction of donors and acceptors is required. The binding energy of the complexes formed between the dopants and the vacancies must be large compared to that of intrinsic Schottky or Frenkel pairs. To assess the impact of doping on electronic transport, the strength of the carrier scattering of the dopant complexes must be compared with that of intrinsic defects and phonons. Furthermore, the dopants should not introduce deep levels that enhance recombination of carriers, if maximum lifetime is desired. The method can be adapted in a straightforward manner to prospect ideal dopants to enhance ionic mobility and reduce electronic mobility in solid electrolytes, for example, or to increase both conductivities for ion battery electrodes or logic switches. Using state of the art quantum mechanical calculations, we analyzed TlBr as a case study since it is an ionic material with excellent electronic properties that degrade over time due to ionic migration. Our results indicate that codoping TlBr with Pb plus Se or S can achieve the desired result, while Te is not a favorable codopant because it introduces a deep trap state. The dopant complexes that form do not significantly affect carrier scattering and electronic mobility. Results using the PBE and HSE06 functionals compared favorably.

This work was performed under the auspices of the U.S. Department of Energy by Lawrence Livermore National Laboratory under Contract No. DE-AC52-07NA27344, with support from the National Nuclear Security Administration Office of Nonproliferation and Verification Research and Development.

*rochaleao1@llnl.gov
†lordi2@llnl.gov

[1] P. Knauth and H. Tuller, J. Am. Ceram. Soc. **85**, 1654 (2002).
[2] F. Esch, S. Fabris, L. Zhou, T. Montini, C. Africh, P. Fornasiero, G. Comelli, and R. Rosei, Science **309**, 752 (2005).
[3] S. Chung, J. Bloking, and Y. Chiang, Nature Mater. **1**, 123 (2002).
[4] B. Bogdanovi and M. Schwickardi, J. Alloys Compd. **253–254**, 1 (1997).
[5] A. Arico, P. Bruce, B. Scrosati, J. Tarascon, and W. Van Schalkwijk, Nature Mater. **4**, 366 (2005).
[6] R. Waser and M. Aono, Nature Mater. **6**, 833 (2007).
[7] S.-Y. Chung, S.-Y. Choi, T. Yamamoto, and Y. Ikuhara, Angew. Chem., Int. Ed. **48**, 543 (2009).
[8] M. Shorohov, M. Kouznetsov, I. Lisitskiy, V. Ivanov, V. Gostilo, and A. Owens, IEEE Trans. Nucl. Sci. **56**, 1855 (2009).
[9] K. Hitomi, M. Matsumoto, O. Muroi, T. Shoji, and Y. Hiratate, IEEE Trans. Nucl. Sci. **49**, 2526 (2002).
[10] K. Hitomi, Y. Kikuchi, T. Shoji, and K. Ishii, IEEE Trans. Nucl. Sci. **56**, 1859 (2009).
[11] A. V. Churilov, G. Ciampi, H. Kim, L. J. Cirignano, W. M. Higgins, F. Olschner, and K. S. Shah, IEEE Trans. Nucl. Sci. **56**, 1875 (2009).
[12] T. Onodera, K. Hitomi, and T. Shoji, IEEE Trans. Nucl. Sci. **54**, 860 (2007).
[13] K. Hitomi, T. Shoji, and Y. Nlizeki, Nucl. Instrum. Methods Phys. Res., Sect. A **585**, 102 (2008).
[14] I. B. Oliveira, F. E. Costa, P. K. Kiyohara, and M. M. Hamada, IEEE Trans. Nucl. Sci. **52**, 2058 (2005).
[15] V. Gostilo, A. Owens, M. Bavdaz, I. Lisjutin, A. Peacock, H. Sipila, and S. Zatoloka, IEEE Trans. Nucl. Sci. **49**, 2513 (2002).
[16] H. Kim, L. Cirignano, A. Churilov, G. Ciampi, W. Higgins, F. Olschner, and K. Shah, IEEE Trans. Nucl. Sci. **56**, 819 (2009).
[17] G. A. Samara, Phys. Rev. B **23**, 575 (1981).
[18] S. R. Bishop, W. Higgins, G. Ciampi, A. Churilov, K. S. Shah, and L. Tuller, J. Electrochem. Soc. **158**, J47 (2011).
[19] Core electrons were treated with the projector augmented-wave method [P. E. Blöchl, Phys. Rev. B **50**, 17953 (1994)]; as implemented in the VASP code [G. Kresse and J. Furthmüller, Phys. Rev. B **54**, 11169 (1996)] and [G. Kresse and J. Furthmüller, Comput. Mater. Sci. **6**, 15 (1996)]. A plane-wave basis set with a cutoff of 320 eV was used, except for calculations involving S and Ca, where 380 eV was used consistently for all systems involved. For Brillouin zone sampling, we used the tetrahedron method with a Monkhorst-Pack mesh of $5 \times 5 \times 5$ and $4 \times 4 \times 4$ k points for the smaller and larger supercell, respectively. The atomic coordinates were relaxed until all residual forces were below 0.01 eV/Å. Some calculations were repeated using the HSE06 hybrid functional [20], which mixes 25% screened Hartree-Fock exact exchange with the PBE functional. All HSE06 calculations used a $3 \times 3 \times 3$ supercell with a $4 \times 4 \times 4$ mesh for sampling the Brillouin zone.
[20] J. Heyd, G. Scuseria, and M. Ernzerhof, J. Chem. Phys. **118**, 8207 (2003).
[21] P. Hohenberg and W. Kohn, Phys. Rev. **136**, B864 (1964).
[22] W. Kohn and L. J. Sham, Phys. Rev. **140**, A1133 (1965).
[23] J. P. Perdew, K. Burke, and M. Ernzerhof, Phys. Rev. Lett. **77**, 3865 (1996).
[24] R. Z. Bachrach and F. C. Brown, Phys. Rev. B **1**, 818 (1970).
[25] L. Grabner, Phys. Rev. B **14**, 2514 (1976).
[26] M.-H. Du, J. Appl. Phys. **108**, 053506 (2010).
[27] See Supplemental Material at http://link.aps.org/supplemental/10.1103/PhysRevLett.108.246604 for comparison of PBE and HSE results and analysis of finite size errors in both approaches.
[28] C. Rocha Leão and V. Lordi, Phys. Rev. B **84**, 165206 (2011).
[29] S. B. Zhang and J. E. Northrup, Phys. Rev. Lett. **67**, 2339 (1991).
[30] G. Makov and M. C. Payne, Phys. Rev. B **51**, 4014 (1995).
[31] More recent methods [32] to treat the issue of spurious electrostatic interactions in periodic systems only differ significantly from Makov-Payne for higher charge states in small supercells.
[32] C. Freysoldt, J. Neugebauer, and C. G. Van de Walle, Phys. Rev. Lett. **102**, 016402 (2009).
[33] Y. Takahashi and E. F. Westrum, J. Chem. Eng. Data **10**, 244 (1965).
[34] C. Persson, Y.-J. Zhao, S. Lany, and A. Zunger, Phys. Rev. B **72**, 035211 (2005).
[35] C. G. Van de Walle and J. Neugebauer, J. Appl. Phys. **95**, 3851 (2004).
[36] The conclusion that Schottky pairs are not bound in [26] ($E_{\mathrm{bind}} = 0.03$ eV) is probably a result of using a small supercell and neglecting Makov-Payne corrections. For a $3 \times 3 \times 3$ cell we obtained $E_{\mathrm{bind}} = -0.05$ eV without the correction and -0.54 eV including it.
[37] T. Kawai, K. Kobayashi, M. Kurita, and Y. Makita, J. Phys. Soc. Jpn. **30**, 1101 (1971).
[38] K. Seeger, *Semiconductor Physics* (Springer, New York, 2004), 9th ed.
[39] G. E. Morse and A. W. Lawson, J. Phys. Chem. Solids **28**, 939 (1967).
[40] J. W. Hodby, H. Tamura, G. T. Jenkin, and K. Kobayashi, Solid State Commun. **10**, 1017 (1972).
[41] C. G. Van de Walle and R. M. Martin, Phys. Rev. Lett. **62**, 2028 (1989).
[42] V. Lordi, P. Erhart, and D. Åberg, Phys. Rev. B **81**, 235204 (2010).